Orihuela, P. M., *et al.*: Preliminary Study on the Performance of Biomorphic…
THERMAL SCIENCE: Year 2018, Vol. 22, No. 5, pp. 2053-2064

2053

PRELIMINARY STUDY ON THE PERFORMANCE OF BIOMORPHIC SILICON CARBIDE AS SUBSTRATE FOR DIESEL PARTICULATE FILTERS

by

Pilar M. ORIHUELA[a*], Aurora GOMEZ-MARTIN
Jose A. BECERRA-VILLANUEVA[a], Javier SERRANO-REYES[a],
Francisco JIMENEZ-ESPADAFOR[a], and Ricardo CHACARTEGUI[a]

[a] Department of Energetic Engineering, University of Seville, Seville, Spain
[b] Department of Condensed Matter Physics, University of Seville, Seville, Spain

This paper presents the results of a preliminary experimental study to assess the performance of biomorphic silicon carbide when used for the abatement of soot particles in the exhaust of Diesel engines. Given its optimal thermal and mechanical properties, silicon carbide is one of the most popular substrates in commercial diesel particulate filters. Biomorphic silicon carbide is known for having, besides, a hierarchical porous microstructure and the possibility of tailoring that microstructure through the selection of a suitable wood precursor. An experimental rig was designed and built to be integrated within an engine test bench that allowed to characterizing small lab-scale biomorphic silicon carbide filter samples. A particle counter was used to measure the particles distribution before and after the samples, while a differential pressure sensor was used to measure their pressure drop during the soot loading process. The experimental campaign yielded promising results: for the flow rate conditions that the measuring devices imposed (1 litre per minute; space velocity = 42,000 L/h), the samples showed initial efficiencies above 80%, pressure drops below 20 mbar, and a low increase in the pressure drop with the soot load which allows to reach almost 100% efficiency with an increase in pressure drop lower than 15%, when the soot load is still less than 0.01 g/L. It shows the potential of this material and the interest for advancing in more complex diesel particle filter designs based on the results of this work.

Key words: *biomorphic silicon carbide, diesel particulate filter,*
particulate matter, soot, filtration efficiency, pressure drop

Introduction

The presence of particles in air has demonstrated to have severe noxious effects on human health and environment [1]. For this reason, the European Commission has already published several Directives setting particles emission limits in Diesel engines: Directive 94/12/EC [2], Directive 98/69/EC [3], Directive 2002/80/EC [4], and Regulation No 715/2007 [5]. Currently, the maximum level allowed of particulate matter emitted by a diesel vehicle is set by the Euro 6 standard [6], and it affects both the number of particles ($6 \cdot 10^{11}$ particles/km) and their mass (4.5 mg/km).

---

* Corresponding author; e-mail: orihuelap@us.es

2054

Orihuela, P. M., *et al.*: Preliminary Study on the Performance of Biomorphic…
THERMAL SCIENCE: Year 2018, Vol. 22, No. 5, pp. 2053-2064

Automotive Diesel engines are an important source of particulate emissions, they emit about ten times more particulate matter than gasoline engines [7]. Although some improvements can be made on the engine to reduce the production of particles, they are not effective enough to meet current regulation [8]. Only the use of after treatment devices has achieved to reduce so far the level of emitted particles down to the thresholds that the standards set. The most extended system for the reduction of particles emissions in diesel vehicles is the wall-flow diesel particulate filter (DPF) [9, 10].

The great awareness of current scientific community about the pollution generated by Diesel engines and the importance of the particulate filters in this kind of vehicles can be seen in the large number of granted patents worldwide related with DPF in the last three years. A quick search in the United States Patent and Trademark Office's database gives 31 results for 2016 with the words *diesel particulate filter* in its abstract, and 45 in 2015.

The DPF can be made from different materials, but silicon carbide (SiC) is currently one of the most popular [11]. Its fundamental properties turn out to be considerably advantageous for commercial filters [12]. The SiC has proven to have high temperature capabilities [13]. Besides having high thermal stability and corrosion resistance, SiC has also higher soot load limit under uncontrolled regeneration than cordierite and aluminum titanate, and thus a lower fuel consumption penalty [14].

The microstructural features of the substrate of a DPF should ensure that the filter has a good performance when applied to a filtration process. Porosity, pore size and permeability are the most influential parameters [13]. In general, the main requirement for a DPF is to have optimum filtration efficiency with the minimum pressure drop [15]. Commercial SiC filters may have initial filtration efficiencies of around 90% [16]. However, the raw materials and the initial processing routes proposed to manufacture of SiC DPF were more expensive than for other materials [13]. That is why a big research effort is being devoted to improve and cheapen the manufacturing process of this kind of filters.

The purpose of this experimental study is to determine the performance of porous biomorphic silicon carbide (bioSiC) as a filter for diesel soot particles in automotive engines. This porous material was presented by De Arellano-Lopez *et al.* [17] as a new low-cost and eco-friendly engineering ceramic material suitable for a considerable range of applications. It has been proved to be suitable for hot gas filtration systems thanks to the microstructure of its interconnected pores and its good mechanical properties [18] even at high temperature as shown by Munoz *et al.* [19] and Varela-Feria *et al.* [20]. Orihuela *et al.* [21] studied the performance of bioSiC as a substrate for soot filters in diesel boilers, and obtained promising results for some precursors. Alonso-Farinas *et al.* [22] developed a candle prototype made of bioSiC, and tested it in a large scale filtration pilot plant providing its suitability as filtration system in integrated gasification combined cycle (IGCC) or pressurized fluidized bed combustion (PFBC) plants.

This study addresses the use of bioceramic filters to remove soot particles from the exhaust gases of Diesel engines, providing for the first time experimental results in a real engine test bench. Previous studies have demonstrated the potential of these materials in other applications. They have been tested for example in the cleaning of hot gases from coal combustion or gasification plants [22], or in the filtration of exhaust gases in a diesel boiler [21]. Also, a recent study of Orihuela *et al.* [23] has demonstrated the reliability of this material in laboratory tests with a soot generator. However, the real operating conditions in the exhaust of an automotive engine are more complex: there is a different gas composition, the temperature and the flow rate are varying, and there may be slight differences in the particle size distribu-

tion respect to an artificial particle generator. This work presents for the first time experimental measurements of the filtration efficiency of two bioSiC specimens when applied to the gas stream of a real automotive engine.

In this way, two disk-shaped samples were manufactured from two different precursors and a particle laden stream extracted from the exhaust pipe of a Diesel engine was used to characterize their efficiency. A test bench was designed and built for this purpose. The transient evolution of the filtration efficiency with the soot load was evaluated through a continuous register of the captured particles, while the pressure drop across the samples was measured with a differential pressure sensor. From this first approach to the application of bioSiC as diesel exhaust particulate filter, positive and promising results are obtained.

Methods

For this study, two bioSiC filters made from different precursors have been tested in the exhaust of a Euro 6 Diesel engine. The precursor selection was made based on a previous characterization stage, in which the most relevant microstructural parameters of a DPF were identified and measured.

The bioSiC filter samples, manufacturing process

In this work, two different bioSiC filters were manufactured: one made from pine, and another one made from medium density fiberboard (MDF) panel. The choice of the precursors was made taking into account those microstructural parameters that are known to affect their performance as particulate filters (porosity, pore size and permeability mainly), and on a previous determination of their filtration efficiency with the exhaust gases of a diesel boiler [21].

In two previous studies, a wide range of precursors' properties were thoroughly characterized particularly in terms of microstructural parameters. The main result of the study can be found in references [24, 25]. In those works, not only different precursors were tried, but they were also tested taking into account the cutting direction of the wood (parallel or perpendicular to the axis of the trunk). Medium density fiberboard and axial-cut pine were finally selected based mainly on their filtration efficiency, but also for practical reasons related with the manufacturing process [23]. Their main features are presented in tab. 1.

Table 1. Measured characteristic parameters of the tested bioSiC samples

	MDF	Pine
Direction of the axis of the sample	Perpendicular to the fibres, parallel to the compaction direction	Parallel to the cells, parallel to the trunk of the tree
Density [gcm^{-3}] [21]	1.73	1.43
Darcian permeability [m^2] [24]	1.0 ($\pm$0.1)$\cdot$10^{-12}	9.4 ($\pm$1.5)$\cdot$10^{-12}
Inertial permeability [m] [24]	2.1 ($\pm$0.8)$\cdot$10^{-8}	11.4 ($\pm$0.7)$\cdot$10^{-8}
Porosity [%] [21]	46	55
Pore size [μm] [21]	3-30	2-50
Specific surface [m^{2}g^{-1}] [21]	0.07	0.09

The samples were manufactured following the fabrication procedure described by Gomez-Martin *et al.* [25]. Only a brief summary is reported here. First, the wood specimens were cut down into blocks and dried in a stove. Then, the wood blocks were paralysed. After that, the resulting carbon blocks were mechanized into disks with 1 inch in diameter and 3

2056

Orihuela, P. M., *et al.*: Preliminary Study on the Performance of Biomorphic…
THERMAL SCIENCE: Year 2018, Vol. 22, No. 5, pp. 2053-2064

mm thick, and infiltrated with molten silicon. Finally, the excess silicon was removed by evaporation at high temperature. Figure 1 shows the final aspect of the samples and two micrographs of their microstructures obtained through SEM, (Jeol 6460 LV), where the difference between their original precursors can be seen. Medium density fiberboard shows a homogenous distribution of the fibres in the horizontal plane, while pine presents separate areas due to the growth rings.

MDF   Pine
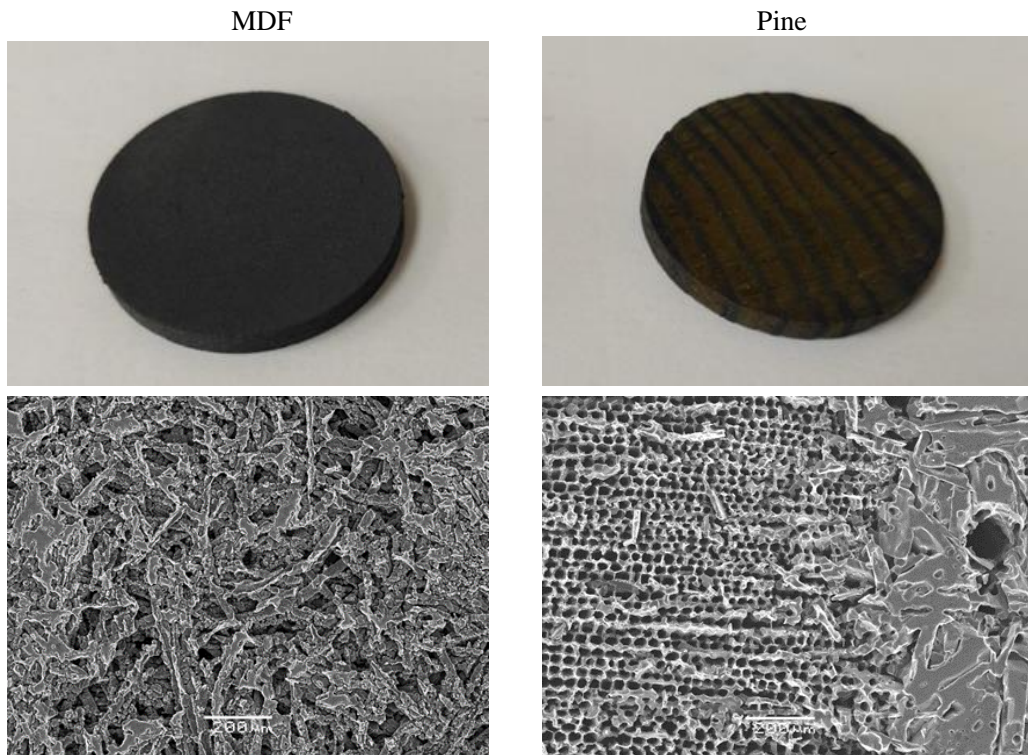
Figure 1. Photos of the filter samples (above), their corresponding micrographs, medium density fiberboard (MDF) sample in the left hand side, pine in the right hand side (below)

Experimental set-up

The aforementioned samples were tested in a bench specifically designed and built to measure their filtration efficiency and pressure drop. The general scheme is depicted in fig. 2.
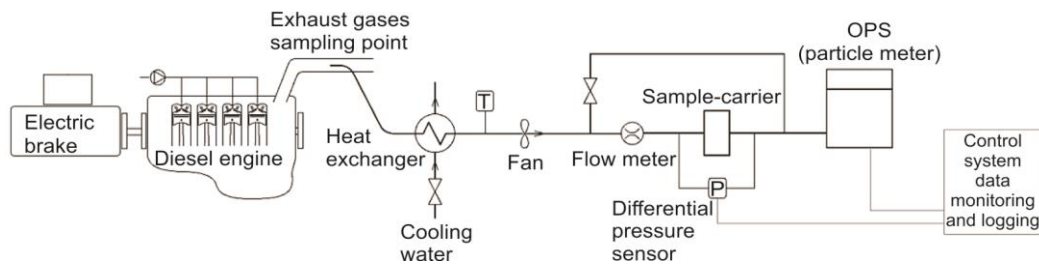
Figure 2. Test rig layout

The particle-laden gas stream used to test the filters is extracted from the exhaust pipe of an 86 hp Diesel engine (2009), the technical features of which are summarized in tab. 2. A fraction of the exhaust gases is deviated from the centre of the exhaust pipe and carried towards the test rig where is filtered with the bioSiC samples. Once fixed to the exhaust pipe, the sampling tube was bent in order to take the sample in the same direction of the flue gases coming from the engine.

A measurement device for particulate emissions (optical particle sizer – OPS) was used to count and measure the concentration of particles before and after placing the filter in the gas stream. Table 3 shows its main technical specifications. The gas-flow rate is set at 1 Lpm by an internal pump of the equipment. A flowmeter placed upstream the sample-carrier was used to check and calibrate the flow. Considering the dimensions and the volume of the samples, this flow rate is equivalent to a space velocity across the filters of 42,000 L/h.

The OPS are devices originally designed to measure ambient air quality and they cannot resist the thermal levels of the exhaust gases of an engine. To cool down the gas stream, a heat exchanger was used. A thermocouple was placed just at the outlet of the heat-exchanger in order to check that the temperature level imposed by the OPS 3330 was not exceeded. Thanks to the previous cooling, the temperature level in the samples during the tests was always below 45 °C.

A small fan is used to compensate the pressure drop introduced by the heat exchanger. In [21], a detailed description of the sample-carrier for the filter samples is provided, and a design sketch and a photo of the same are presented. A differential pressure sensor (Honeywell 24PC 0.5 psi) was used to measure the pressure drop in the filter during the soot load.

Table 2. Technical specifications of the engine

Renault Clio III, 1.5 TDI	
Manufacturer, Model	Renault, Clio III
Type	K9K766
Power	86 hp
Number of cylinders	4
Displacement	1461 cm^3
Injection system	Diesel common-rail
Pressure ratio	17.9
Manufacturing year	2009
Emission standard	Euro IV

Table 3. Technical specifications of the particle sizer

The OPS 3330	
Manufacturer	TSI
Model	OPS 3330
Measurement principle	120° light scatter
Flow rate	1 Lpm ±5%
Sampling time	≥1 second
Particle size range	0.3 to 10 μm
Channels no.	16
Size resolution	5% at 0.5 μm
Particle concentration limit	3,000 particle/cm^3
Mass concentration	0.001 to 275,000 μg/m^3

The monitoring and logging of the data measured with the particle meter and the pressure sensor were done remotely from outside the engine cell with data acquisition system and control software. The test cell of the engine is prepared to perform tests in different injection modes and with different types of fuel. A fuel delivery regulator and an electric brake control the engine speed and the load independently. The brake moment was determined by a gauge. The filtration tests of this study were carried out controlling the engine working point at 2,500 rpm and 70 Nm, a frequent operation regime in experimental campaigns with this kind of engines. Before placing any filter, the engine was left operating during at least one hour, warming up, in order to assure steady-state conditions. However, in the initial stage, a

previous characterization of the distribution of particles as a function of the operation regime was performed.

In fig. 3 two pictures of the experimental facility are presented. On the left hand side, one picture of the engine is shown, and in the right hand side, another one of the test rig.
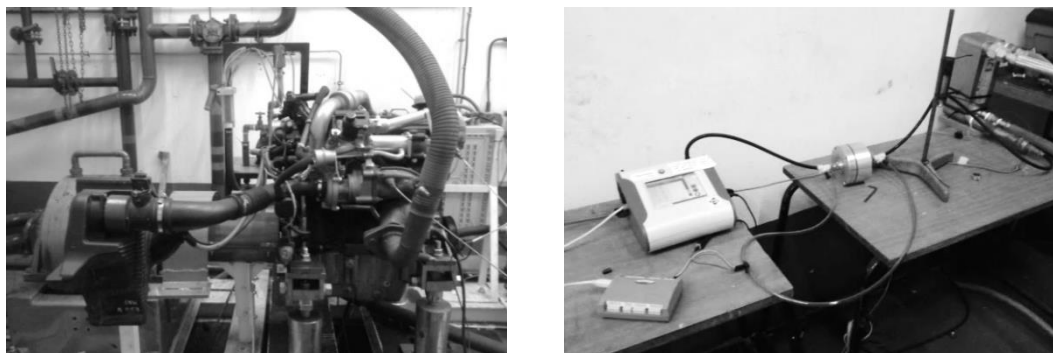
Figure 3. Photos of the experimental facility; the automotive Diesel engine (left) and the test rig (right)

The heat exchanger may affect considerably the particle size distribution of the gas. In addition to following a tortuous path, gases experience a quick cooling during it crossing across the heat exchanger. The cooling of a particle laden gas stream causes the nucleation and condensation of volatile materials, and also the formation of bigger agglomerates by the coagulation of particles [26]. Furthermore, the temperature gradients near the cold walls are known to cause the movement of the particles by thermophoresis [27]. Due to these phenomena the particle distribution downstream the heat exchanger can be altered respect to the original distribution generated by the engine. This alteration on the particle size distribution was kept in mind during the design and the assembling of the test bench. Nevertheless, it should not affect the efficiency calculations since the measurements of the concentration of particles were made just before and just after the place of the filter.

Calculation procedure

The filtration efficiency of each sample was calculated from the measurements of particle concentration before and after the filter. The calculation procedure can be found in [21].

Up to 16 channels were set in the OPS 3330 to take into account different particle size ranges: from 300 nm, the minimum diameter detectable by the device, to 1,500 nm. The distribution of sizes on the OPS is set logarithmically as shown in tab. 4.

The logging time was set to 1 second in order to accurately measure the transient evolution of the filtration efficiency with the soot load. The length of the tests was determined by the capability of the measuring device to keep the pump on. The OPS 3330 needs a free path for the air to flow into it. When a blockage starts hindering the flow, the pump cannot continue sucking and the device stops measuring to avoid contaminating the optical chamber.

The evolution in the filtration efficiency of each sample was calculated during the test and expressed as a function of the time and the soot load. Local oscillations of the curves were smoothed by averaging the calculated values of efficiency every 120 seconds. To calculate the deposited soot load on the samples in each moment, the calculation procedure described in [21] was used. Soot particles produced by Diesel engines are known to form fractal-shaped agglomerates [28], and they are characterized by their mobility diameter. The mo-

Orihuela, P. M., *et al.*: Preliminary Study on the Performance of Biomorphic…
THERMAL SCIENCE: Year 2018, Vol. 22, No. 5, pp. 2053-2064

2059

bility diameter cannot be directly inferred from the optical diameter unless any merging technique with other kind of sizer (SMPS or DMA) is used [29]. However, in this study, the optical diameter was used for the mass calculations, and awareness of the lack of quantitative validity of the results was assumed.

**Table 4. Particle size arrangement in the channels of the OPS: diameter range,
logarithmic mean diameter (LMD), and effective density**

	Channel							
	1	2	3	4	5	6	7	8
Lower diameter [nm]	300	317	335	354	374	395	417	440
Upper diameter [nm]	317	335	354	374	395	417	440	465
LMD [nm]	308	326	344	364	384	406	428	452
Effective density [gcm^{-3}]	0.867	0.834	0.803	0.772	0.743	0.716	0.689	0.663
	Channel							
	9	10	11	12	13	14	15	16
Lower diameter [nm]	465	491	519	548	579	612	700	1500
Upper diameter [nm]	491	519	548	579	612	700	1,500	10,000
LMD [nm]	478	505	533	563	595	656	1,100	5,750
Effective density [gcm^{-3}]	0.638	0.614	0.591	0.569	0.547	0.489	0.287	0.076

The effective density was calculated using the correlation proposed by [30] for fractal like soot particles produced by Diesel engines:

$$\rho_e = \rho_0 \left(\frac{d_m}{d_0} \right)^{D_f - 3} \tag{1}$$

where d_0 and ρ_0 are the primary particle diameter and density, respectively, and D_f is the fractal dimension. Orihuela *et al.* [21] outline acceptable values for these parameters: $d_0 = 60$ nm and $\rho_0 = 0.7$ g/cm^3 from [28], and $D_f = 2.3$ from [28] and [30]. The effective density of the particles in each size range is also showed in tab. 4. As stated by Park *et al.* [31], the higher the diameter of an agglomerate, the lower the resulting effective density due to the increasing presence of voids.

Results

The filtration tests were carried out with the engine working at 2,500 rpm and 70 Nm, a frequent operation regime in experimental campaigns with this kind of engines. In this regime, as in any other, the range of particle diameters detectable by the particle counter corresponds to the final part of the complete particle distribution curve of a normal automotive engine. That is, the production of particles of a normal engine starts usually from much smaller particles, around 1 nm. To obtain the whole curve of particle distribution, a device capable to detect particles of few nanometres would be necessary. Optical meters only detect particles above 300 nm, and so they cannot reflect the complete particle distribution curve of an engine.

Consequently, the values of filtration efficiency obtained from this study and presented in this paper are applicable to particles above 300 nm, but cannot be applicable to smaller particles. To get a complete value of the filtration efficiency of the filter samples for the whole range of sizes, further study would be necessary, and a different kind of particle meter would be required.

Apart from the limitation on the measurable particle sizes, an alteration of the particle size distribution may exist in respect to the original distribution of the engine, due to the cooling process in the heat exchanger. This effect should not affect the efficiency calculations since the measurements of the concentration of particles were all made downstream the heat exchanger, just before and after placing the filter.
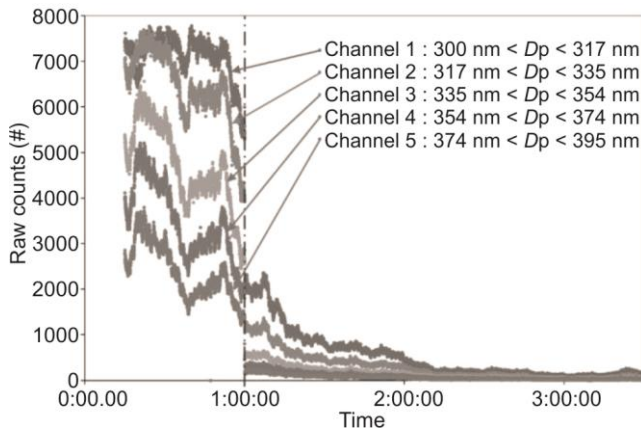
Figure 4. Evolution in the number of particles (raw count) during one filtration test for different particle sizes
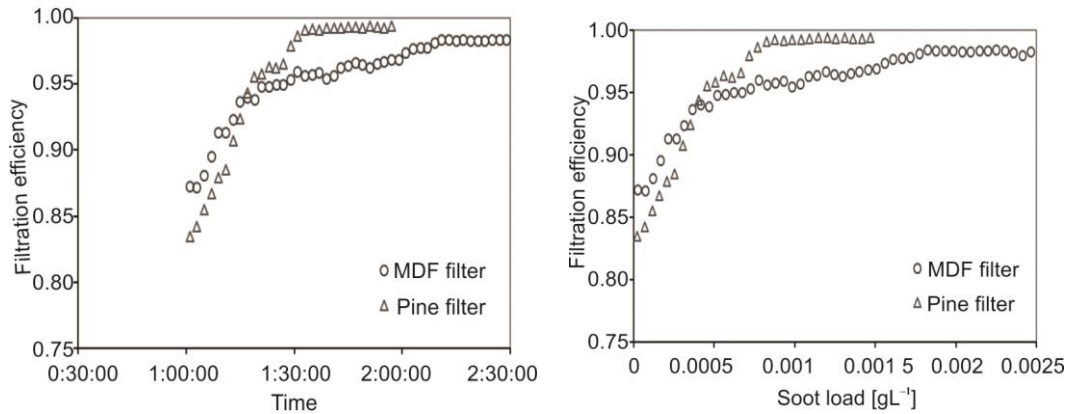
Filtration efficiency

Figure 4 shows the evolution in the measured amount of particles during one filtration test, in particular during the MDF sample filtration test. In the figure, the raw count of particles is presented as a function of the time for five different size ranges (corresponding to channels 1 to 5, see tab. 4).

The first 45 minutes of the graph correspond to the time period in which the gas stream is not being filtered, that is, before placing the filter sample. In the instant in which the filter is placed in the sample-carrier, a sudden decrease in the number of particles is recorded. This instant determines the initial filtration efficiency of the bioSiC filter, that is, the efficiency of the clean filter when it has not been loaded with particles yet. From then on, a continuous decrease in the measured number of particles is observed. The particles trapped within the filter contribute in turn to improve the abatement efficiency. Eventually, the pores get saturated and no more particles achieve to cross the filter. In that moment, the filtration efficiency of the filter reaches a maximum value close to 100%.
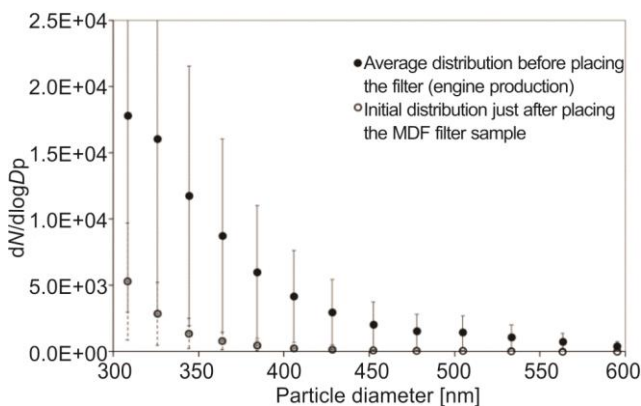
Figure 5. Reduction in the particle distribution curve for the moment in which the MDF filter sample starts filtrating

The rapid decrease in the number of particles that takes place in the moment the filter is placed can also be observed in the particle distribution curves. Figure 5 shows the averaged particle distribution before placing the filter, and the one obtained just after placing it. Averaging this initial reduction in the number of particles for all the size ranges, the initial efficiency of the filters was obtained. The result was 86% for the MDF, and 83% for pine.

Plotting the following evolution of the filtration efficiency from then on for the rest of the test, the results shown in fig. 6 were obtained. In this figure, trends have been plotted for both MDF and pine sample. It can be seen that the initial efficiency of

Orihuela, P. M., *et al.*: Preliminary Study on the Performance of Biomorphic…
THERMAL SCIENCE: Year 2018, Vol. 22, No. 5, pp. 2053-2064

2061

pine is a bit lower than that of MDF, but the growing rate is higher so it surpasses the curve of MDF and reaches sooner 100% efficiency.
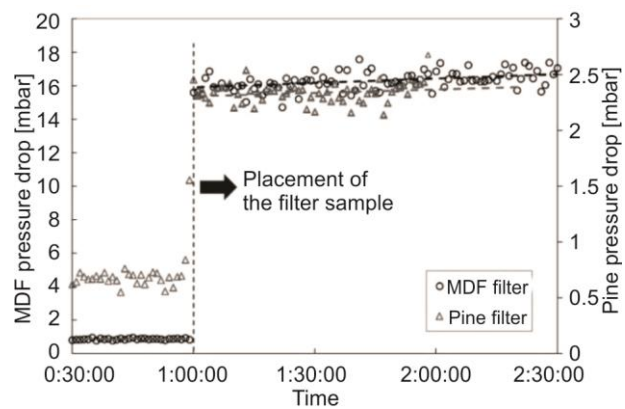

Figure 6. Filtration efficiency of the bioSiC filters as a function of the soot load and the time
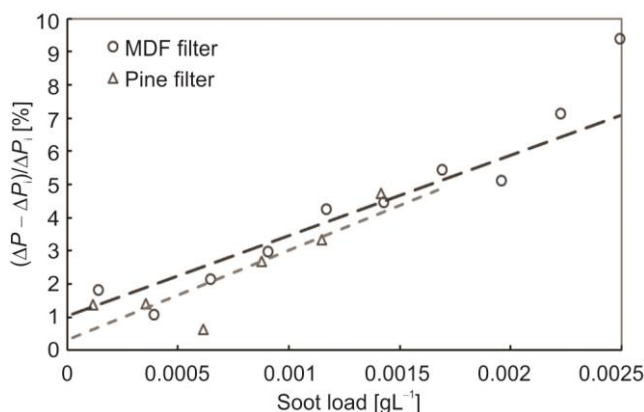
Pressure drop

The pressure drop was measured throughout the tests including the first time period in which the engine was warming up and the filters had not been placed yet. In that stage, a little pressure drop was measured due to the pipes and the sample-carrier itself. That pressure drop is around 0.5 mbar and is independent from the filter sample as can be seen in fig. 7. In the moment the sample is placed, a sudden increase in pressure drop is registered. The initial pressure drop of the MDF filter is higher than the one of the pine filter. This initial pressure drop corresponds to the pressure drop of a clean filter and matches with the expectable pressure drop of a bioSiC filter according to its permeability.

From the moment the filter is placed blocking the gas stream, it starts getting loaded with soot particles. Captured particles remain on the surface of the pores reducing the effective cross sectional area for the air-flow and increasing the pressure drop, fig. 8. If the filtration process is long enough the pores of the filter get eventually clogged, and a soot cake starts forming on the external surface of the filter. In this experiment, the tests stopped before the soot cake appeared due to the quick evolution in the filtration efficiency of the samples, which raised up to almost 100% for an increase in pressure drop less than 15%.

Unfortunately, the blockage of the gas flux at the beginning of the soot cake formation interfered with the proper operation of the internal pump of the OPS, so the measurement and data logging were stopped before reaching a significant increase in the pressure drop.

Figure 7. Pressure drop of the bioSiC filters as a function of the time

2062

Orihuela, P. M., *et al.*: Preliminary Study on the Performance of Biomorphic…
THERMAL SCIENCE: Year 2018, Vol. 22, No. 5, pp. 2053-2064

Figure 8. Increase in pressure drop (percentage) as a function of the soot load

Conclusions

Through this study, the filtration performance of bio SiC as DPF has been addressed. In this preliminary study, two different filters samples made from two different wood precursors have been tested: one made from MDF, and another one made from Pine. In a previous study, these precursors had demonstrated to have suitable microstructural parameters for their use as substrate for particle filters [32]. The cutting direction of a natural wood is also a crucial element in the interaction of the resulting porous microstructure and the soot laden air-flow [21]. Thus, the pine-derived bioSiC sample was manufactured following the cutting direction that better filtration efficiency might provide, that is, axial (air flowing parallel to the trunk of the tree). The manufacturing process followed here was the same process used by Gomez-Martin *et al.* [24, 25], which in turn follows the same guidelines than other manufacturing processes of bioSiC described previously in the literature.

To test the bioSiC filter samples, a test rig was specifically designed and built in which a four cylinder, turbocharged, common-rail injection, 1.461 L Renault DI automotive Diesel engine was used to generate the soot laden gas stream to be filtered. To measure the concentration of particles before and after placing the filter samples, and to be able to calculate the filtration efficiency, an optical particle sizer was used. Simultaneously, a differential pressure sensor was used to measure the pressure drop in the filters as they got loaded with soot.

The initial filtration efficiency of both samples is higher than 80% : 86% in the case of MDF and 83% in the case of pine. This filtration efficiency increases even more as the filters get loaded with particles, reaching efficiencies close to 100% in a period shorter than 2 hours (for a space velocity of around 42000 1/h). As expected, this increase in the filtration efficiency is accompanied by an increase in pressure drop. Nevertheless, filtration efficiency has turned out to reach its maximum value before the increase in pressure drop reaches a 15%.

The study has revealed two main limitations:
(1) the particle size range of the measuring device (OPS 3330) does not allow to register the complete size distribution curve. The results obtained through this study are applicable to particles larger than 300 nm, and
(2) the blockage of the flux stopped the measurements before the soot cake started to form, so a bias pressure drop curve is obtained.

Both limitations could be solved by using a different particle meter like, for example, an SMPS. In any case, although preliminary, results obtained in this work are positive and encourage further studies with more complex geometries and extended tests. In this sense, further researches are required to extend the validity to the nanoscale range, since nanoparticles have demonstrated to be especially harmful and dangerous for human health. Besides, longer tests would be necessary in order to study the soot cake filtration stage. In the meanwhile, bioSiC may be considered a suitable candidate for its use as substrate for DPF.

For future research, other filtration conditions could be studied. By using a laminar diffusion flame, for example, a well-known particle concentration and distribution could be obtained, and a more systematic and accurate measurement of the filtration efficiency could be done. In addition, to characterize the soot distribution, some laser diagnostic technics could be used, which would be more affordable than purchasing more sophisticated equipment to sample, count and classify particles.

Acknowledgment

References

[1] Prasad, R., Bella, V. R., A Review on Diesel Soot Emission, its Effect and Control, *Bull. Chem. React. Eng. Catal.*, *5* (2010), 2, pp. 69-86
[2] ***, Directive 94/12/EC, Off. J. Eur. Comm. 100, pp. 42-52, 1994
[3] ***, Directive 98/69/EC, Off. J. Eur. Comm. 350, pp. 1-56, 1998
[4] ***, Directive 2002/80/EC, Off. J. Eur. Comm. 291, pp. 20-56, 2002
[5] ***, Regulation No. 715/2007, Off. J. Eur. Comm. 1716, pp 1-16, 2007
[6] ***, Regulation No. 459/2012, Off. J. Eur. Comm. 142, pp. 16-24, 2012
[7] Martirosyan, K. S., *et al.*, Behavior Features of Soot Combustion in Diesel Particulate Filter, *Chem. Eng. Sci.*, *65* (2010), 1, pp. 42-46
[8] Neeft, J. P. A., *et al.*, Diesel Particulate Emission Control, *Fuel Process. Technol.*, *47* (1996), 1, pp. 1-69
[9] Howitt, J. S., Montierth, M. R., Cellular Ceramic Diesel Particulate Filter, *SAE Transactions*, *90* (1981), Section 1: 810010-810234, pp. 493-501
[10] Guan, B., *et al.*, Review of the State-of-the-art of Exhaust Particulate Filter Technology in Internal Combustion Engines, *J. Environ. Manage.*, *154* (2015), May, pp. 225-258
[11] Adler, J., Ceramic Diesel Particulate Filters, *Int. J. Appl. Ceram. Technol.*, 2 (2005), 6, pp. 429-439
[12] Ohno, K., *et al.*, Characterization of SiC-DPF for Passenger Car, SAE technical paper, 2000-01-0185, 2000
[13] Young, D., *et al.*, Silicon Carbide for Diesel Particulate Filter Applications: Material Development and Thermal Design, SAE technical paper, 2002-01-0324, 2002
[14] Millo, F., *et al.*, Impact on Vehicle Fuel Economy of the Soot Loading on Diesel Particulate Filters Made of Different Substrate Materials, *Energy*, *86* (2015), June, pp. 19-30
[15] Petasch, U., Adler, J., Diesel Particulate Filters with Optimized Pressure Drop and Filtration Efficiency, Fraunhofer IKTS Annual Report 2013/14, Fraunhofer Institute for Ceramic Technologies and Systems IKTS, Dresden, Germany, 2014
[16] Yang, J., *et al.*, Single Wall Diesel Particulate Filter (DPF) Filtration Efficiency Studies Using Laboratory Generated Particles, *Chem. Eng. Sci.*, *64* (2009), 8, pp. 1625-1634
[17] De Arellano-Lopez, A. R., *et al.*, Biomorphic SiC: A New Engineering Ceramic Material, *Int. J. Appl. Ceram. Technol.*, *1* (2005), 1, pp. 56-67
[18] Bautista, M. A., *et al.*, Microstructural and Mechanical Evaluation of Porous Biomorphic Silicon Carbide for High Temperature Filtering Applications, *J. Eur. Ceram. Soc.*, *31* (2011), 7, pp. 1325-1332
[19] Munoz, A., *et al.*, High Temperature Compressive Mechanical Behavior of Joined Biomorphic Silicon Carbide Ceramics, *J. Eur. Ceram. Soc.*, *22* (2002), 14-15, pp. 2727-2733
[20] Varela-Feria, F. M., *et al.*, Low Density Biomorphic Silicon Carbide: Microstructure and Mechanical Properties, *J. Eur. Ceram. Soc.*, *22* (2002), 14-15, pp. 2719-2725
[21] Orihuela, M. P., *et al.*, Performance of Biomorphic Silicon Carbide as Particulate Filter in Diesel Boilers, *J. Environ. Manage.*, *203* (2017), Part 3, pp. 907-919

[22] Alonso-Farinas, B., *et al.*, New Candle Prototype for Hot Gas Filtration Industrial Applications, *Fuel*, *114* (2013), Dec., pp. 120-127

[23] Orihuela, M. P., *et al.*, Experimental Measurement of the Filtration Efficiency and Pressure Drop of Wall-flow Diesel Particulate Filters (DPF) Made of Biomorphic Silicon Carbide Using Laboratory Generated Particles, *Appl. Therm. Eng.*, *131* (2018), Feb., pp. 41-53

[24] Gomez-Martin, A., *et al.*, Permeability and Mechanical Integrity of Porous Biomorphic SiC Ceramics for Application as Hot-gas Filters, *Mater. Des.*, *107* (2016), Oct., pp. 450-460

[25] Gomez-Martin, A., *et al.*, Thermal Conductivity of Porous Biomorphic SiC Derived from Wood Precursors, *Ceram. Int.*, *42* (2016), 14, pp. 16220-16229

[26] Ning, Z., *et al.*, Experimental Investigation of the Effect of Exhaust Gas Cooling on Diesel Particulate, *J. Aerosol Sci.*, *35* (2004), 3, pp. 333-345

[27] Strom, H., Sasic, S., The Role of Thermophoresis in Trapping of Diesel and Gasoline Particulate Matter, *Catal. Today.*, *188* (2012), 1, pp. 14-23

[28] Matti Maricq, M., Chemical Characterization of Particulate Emissions from Diesel Engines: A Review, *J. Aerosol Sci.*, *38* (2007), 11, pp. 1079-1118

[29] Tritscher, T., *et al.*, Data Merging of Size Distributions from Electrical Mobility and Optical Measurements, in: *Europen Aerosol Conference Handbook*, Prague, 2013

[30] DeCarlo, P. F., *et al.*, Particle Morphology and Density Characterization by Combined Mobility and Aerodynamic Diameter Measurements, Part 1 Theory, *Aerosol Sci. Technol.*, *38* (2004), 12, pp. 1185-1205

[31] Park, K., *et al.*, Relationship between Particle Mass and Mobility for Diesel Exhaust Particles, *Environ. Sci. Technol.*, *37* (2003), 3, pp. 577-583

[32] Orihuela, M. P., *et al.*, Behavior of Biomorphic SiC as a Particulate Filter in Automotive Diesel Engines (in Spanish), LV Congress of the Spanich Society of Ceramics and Glass, Seville, Spain, 2016